Commissioning report of the nights 27-29 of August 2002 used for the Coronographic Mask Device for the A/O System at the WHT: OSCA

compiled by S.G. Els*& P. Jolley

19. September 2002

1 Intention of this document

This document is intended to provide technical informations about the coronographic mask device OSCA at the WHT. The presented data have mainly been obtained during the two commissioning nights between 27 and 28 of August 2002 on sky.

A calibration plan for OSCA is outlined at the end of this document. If realized updated performance and calibration numbers will be provided on the ING webpages (http://www.ing.iac.es) frequently.

2 System Overview

OSCA (Optimized Stellar Coronograph for Adaptive Optics) is a coronographic mask device designed to be used in combination with the adaptive optics (A/O) system NAOMI which is mounted in the Nasmyth focus of the 4.2m Wilhelm Herschel Telescope (WHT) on La Palma. It was built at the Optical Science Laboratory of the University College London (UCL) by Peter Doel.

OSCA is placed in front of the science detector which at present is the infrared camera INGRID. In the future (from 2003 on) it is intended to also be used in combination with the integral field spectrograph OASIS.

Via mirrors the light beam coming from the NAONI A/O system is sent on the focal plane mask and then reimaged on the science camera. The whole OSCA device is mounted in a way that it can be moved in and out of the light beam remotely within approximatly 30 seconds. There are currently 6 different masks installed. The observer can choose via a GUI the mask of choice which then moves into the light path. This configuration is intended to give maximum flexibility to the observer which mask size to use for given atmospheric conditions.

The focal plane masks are vaporized onto substrates and are mounted into a mask wheel. In this way diffraction patterns produced by possible holders of the masks are avoided. The currently installed masks and their sizes are given in Table 1.

*supported under Marie-Curie Fellowship contract HPMD-CT-2000-00005.

3 Technical Report

OSCA had been installed and first commissioned end of May 2002. The main funcionalities have been tested off– and on–sky. The system has been shown to work reliable, i.e., deploying with good reproducibility and stability of the system on short time scales. Even though not officially offered to the user a few science programmes already made use of OSCA. This is due to the quick and easy way of deploying OSCA into the light beam.

A re–alignment of the whole A/O system NAOMI–OSCA–INGRID has been taken place before the end of August 2002 meaning that previous obtained performance estimates have to be updated.

The here presented on–sky data have been obtained during the two nights between 27–29 of August 2002. Due to technical problems of the adaptive optics system the first of those nights was, except for 2.5 hours at the end of the night, lost. The data obtained at the end of the second night suffered from clouds. Off–sky data are all only used to obtain "relative" measurements meaning that such measurements are not affected by alignement changes.

3.1 OSCA field of view (FOV)

In Figure 1 the FOV of OSCA is seen by observing dome flatfields. The FOV is a circular part of the NAOMI FOV with a diameter of $\sim 30''$on sky. In the centre of the FOV the mask is localized. Some vignetting is present towards the left hand side of the FOV which affects the outer $6''$. The cause of this vignetting is currently unknown. But as this vigneting is present in the data obtained during May 2002 as well in data taken during August 2002 this means that this vignetting is independent from different alignments.

In order to obtain the plate scale and orientation of the FOV the Trapezium cluster was observed as astrometric reference field. These data suffer badly from clouds. However, a comparison of the relative positions of stars in that cluster observed with and without OSCA show that the FOV with OSCA is inverted as compared to NAOMI alone, i.e. with OSCA north is up and east to the left.

The plate scale stays constant with and without OSCA (as it was designed to be) within 2–5%.

An analysis of the data to obtain an absolute platescale of OSCA and also its orientation on the sky is ongoing. Such astrometric measurements and monitoring of the system are very important especially in the case of coronography: confirmations of possible companions require precise astrometry in order to check for common proper motion pairs. Therefore frequent observations of an astrometric reference field are required.

3.2 Flatfields

OSCA consists of several optical surfaces which first put the focussed beam on the focal plane mask and then refocus the beam onto the science detector. All these surfaces will modify the flatfield behaviour. Therefore science observations using OSCA should always be flatfielded with flatfields taken in the same OSCA configuration as the science images. Fig.1 shows dome flatfields taken with the different OSCA focal plane masks (except the $0\overset{''}{.}2$ mask). The most obvious effect will come from dust grains and/or dirt. The substrates on which the masks have been vaporized on are located in the focal plane. Therefore every dust grain located on these substrates will be perfectly imaged onto INGRID. In Fig. 1 it is clearly seen that dust particles are present on most of the masks. Especially on the $0\overset{''}{.}4$ mask a lot of dirt is visible and a substantial cleaning should be done soon.

This demonstrates the need for a proper enclosure or dust cover for OSCA and also of a regular monitoring of the focal plane masks for contanination and/or degradation of the substrates.

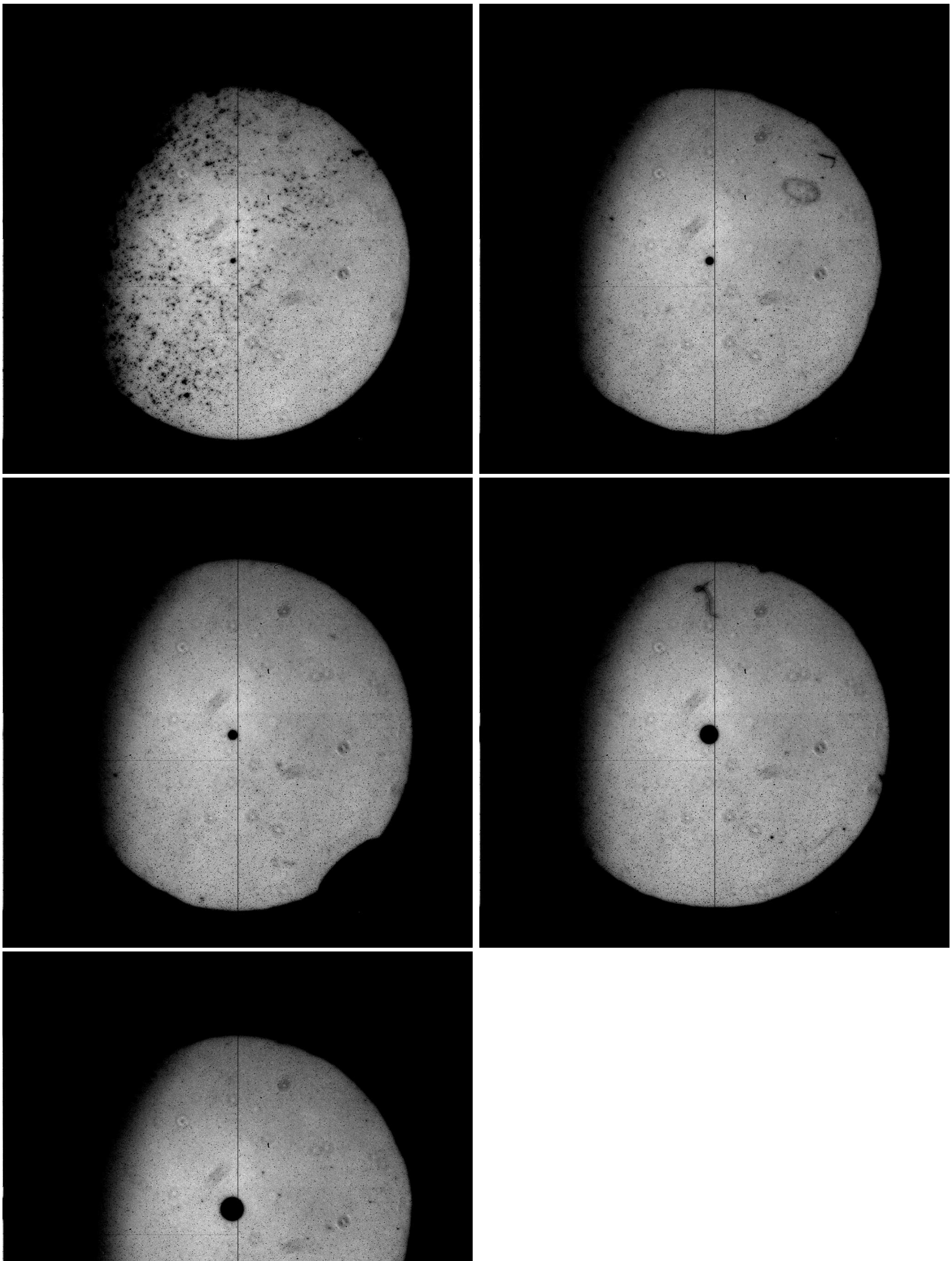

Figure 1 Flatfields taken through OSCA in H band. From top left to bottom the $0.''4$, $0.''65$, $0.''8$, $1.''6$ and $2.''0$ masks are shown. All images are scaled linearly between 0.7 and 1.2. The ring like features apparent in all images are not caused by OSCA.

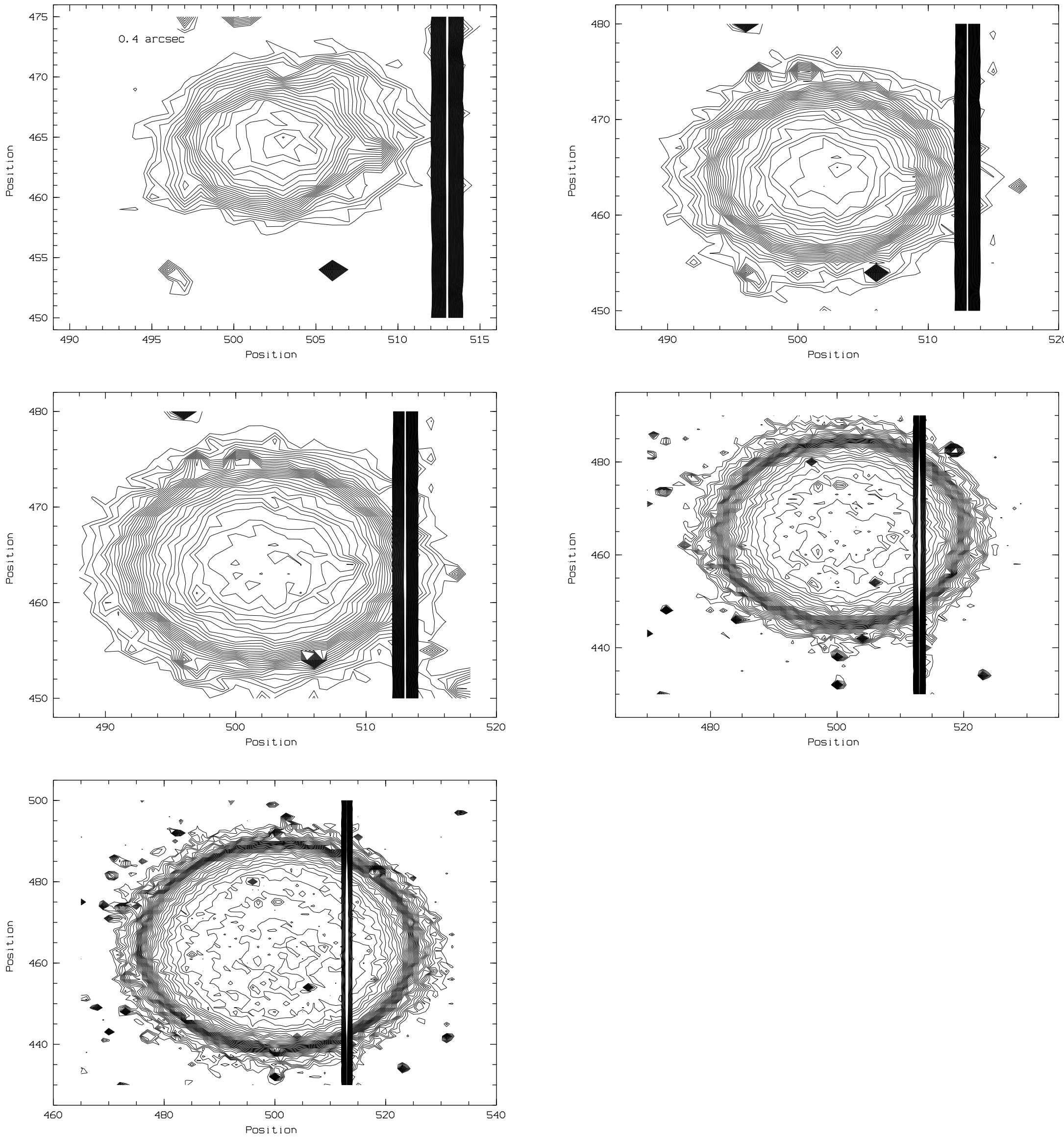

Figure 2 Contour maps of the individual masks. From top left to bottom right the 0.″4, 0.″65, 0.″8, 1.″6 and 2.″0 masks are shown. The edges of the masks extend over 2-3 pixels. This will affect the detection limits of the smallest masks as this corresponds already to a significant part of their total size. The black bar towards the right side indicates the quadrant boundary of the INGRID CCD which is 2 pixels broad.

3.3 Properties of individual masks

The masks are vaporized onto substrates. These substrates are all mounted in a wheel which allows to move one substrate (mask) into the beam at the focal plane of NAOMI. Their geometry is circular with the individual parameters given in table 1. Note that the measured sizes and opacities of the masks depend on their homogeneity. The presented values are an average size between the pixel at which maximum opacity and no opacity occurs. A final definition of the mask size has to be developed.

Figure 2 shows the contours of the 0.″4 to 2″masks. It can be seen that the edges of the masks extend over 2–3 pixels. This especially affects the masks with sizes <0.″8 and leads to the higher error in the determination of the overall opacity of this mask. If this affects

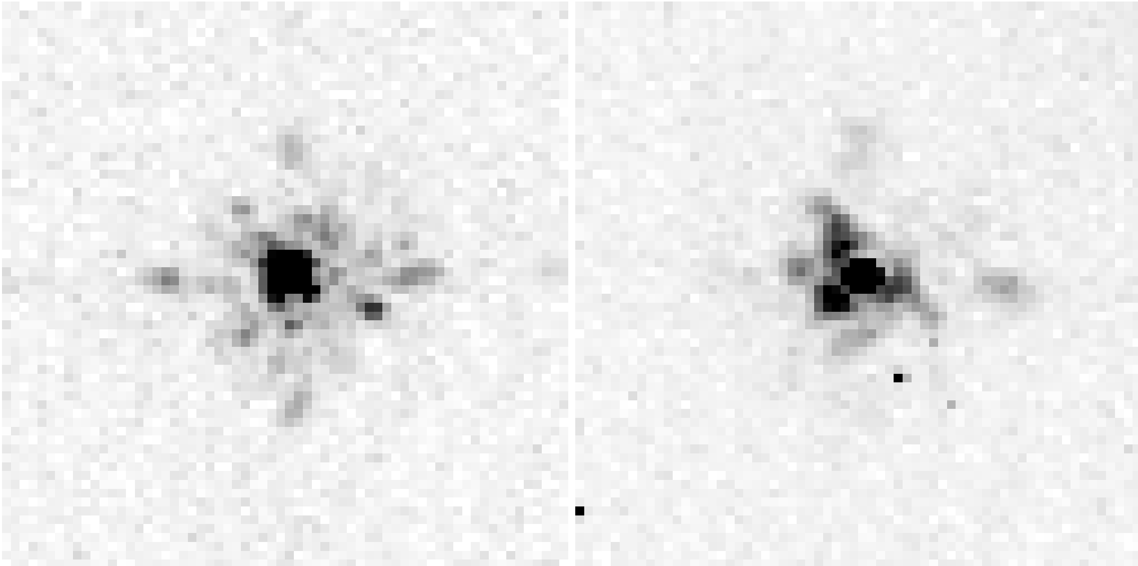

Figure 3
Images of an artificial star (pinhole). Left: the image after simplexing on INGRID in H. Right: same setup as left but OSCA has been deployed. The target mask was used to obtain this image.

also the detection limits is not clear yet and has to be further investigated but it was found that centering of either a star or the pinhole image is very difficult on these masks.

The optical densities (opacity/"Neutral density") of the individual masks have been originally measured by the OSCA team in the laboratory of UCL using a 630 nm Laser. These optical ND values are listed in table 1. To obtain the infrared opacities of the stops an image of the pinhole (artifical star) was put behind the individual stops and then imaged on INGRID. This has only been done for the 0.″8 and 2″masks so far. It is mandatory to obtain these values also for the other stops in the future when a new movable pinhole is available. It turns out that the optical density of the stops is decreasing in the IR by an order of magnitude as compared to their density in the optical.

Also it should be noted that the measurements of the density of the smallest masks is very difficult as the centering is getting difficult as the extension of the edges of these stops becomes comparable to their size.

3.4 AO performance / Introduction of static abberations

During the setup of the NAOMI an iterative procedure (a simplex algorithm) is done in order to obtain a DM shape which compensates for non-common path errors (static

mask	measured diameter (arcsec)	measured opacity 630 nm[1] / J / H / K_S
0.″25		ND 4.5
0.″40	0.″38	ND 4.5
0.″65	0.″68	ND 3.5 / 2.1 / 2.1 / 1.8
0.″80	0.″77	ND 3.5
1.″60	1.″71	ND 3.5
2.″00	1.″95	ND 4.5 / 2.4 / 2.1 / 1.9

Table 1
Measured mask parameters as appearing on INGRID. The uncertainty of the sizes is ±2 pixel, corresponding to 0″08 (assuming the NAOMI-INGRID platescale).
[1]Values of supression in the optical domain provided by UCL.

abberations) between the light beams seen by INGRID and the WFS. Such abberations are thus introduced after the light has passed the dichroic.

As the the focal plane masks of OSCA are on substrates and the lightbeam thus has to pass through them this will introduce static abberations. It is noteworthy that the substrates on which the masks are located are wedged.

As can be seen in Fig.3 OSCA introduces singificant static abberations. The optimum PSF obtained by the simplex process (Fig.3, left) shows a strong single peak surrounded by some cross shaped structure which is introduced by the fully segmented DM. Moving OSCA into the beam changes this PSF significantly (Fig.3, right).

The Strehl-ratio of this image has degraded by 62% as compared to the image taken without OSCA.

It is therefore mandatory in the future to also run the simplex procedure through OSCA before a night during which OSCA is going to be used.

The presented images have been taken through the $1''$target mask. This mask has a crosshair in its center. No comparison of static abberations between the individual masks have been done. But for practial reasons as well as the optical surfaces of the different substrates are supposed to be very similar the simplex through OSCA should be done using the $1''$target mask. Also the wedged structure of the substrates make simplexing only useful at the actual position of the masks which in turn is only accessable by using the $1''$target.

If the abberations introduced by OSCA are stable has not been verified yet. Therefore OSCA should be deployed several times and changes of the PSF should be monitored.

3.5 Photometric zeropoints

Observations of the photometric standart star SAO054271 were obtained during the night from 28-29 of August 2002 positioned several arcseconds away from the $1\farcs6$ mask. The measured zeropoints are listed in Table 2. The zeropoints of the different substrates (masks) have not been determined yet.

date	substrate	standart star	Z_J	Z_H	Z_{Ks}
28.08.02	$1\farcs6$	SAO054271	21.42 (0.05)	21.67 (0.05)	20.99 (0.07)

Table 2 Measured zeropoints ($Z_{J,H,Ks}$) of INGRID in combination with NAOMI and OSCA. The $1\farcs6$ mask was used.

During the night 27-28 of August the same photometric standart was observed also without OSCA but only in H band. The found zeropoint here is $Z_H = 22.50$. Comparing the various configurations in which INGRID can be used the following relative (to INGRID at Cassegrain) efficencies are obtained:

Configuration	Throughput in J	H	K_S
INGRID at Cass	100%	100%	100%
INGRID + NAOMI:		42%	
INGRID +OSCA + NAOMI	17%	20%	21%

The factor 2 between the NAOMI and NAOMI+OSCA throughput is expected because of the OSCA Lyotstop. A second Lyotstop is available and a new holder for the Lyotstops will be installed soon enabling the selection of the Lyotstop of choice (bigger/smaller stop) before a night.

3.6 On-sky PSF suppression

To obtain an estimation of the performance of the whole system a bright object with H=8 was observed with several masks. During that night the Lyostop rotation was not functioning and therefore some residual scattered light from the telescope secondary spider is visible on the images. These areas were avoided when measuring the final detectivity.

In Figures 4 and 5 the final sensitivities of the 0.″8 and 1.″6 masks are shown. The detectivity in the region close to the bright object is limited by photon noise. The transition region between which photon noise and readout noise limit occurs lies theoretically between 2″and 3″. The detection limit close to a bright object is thus only dependent on the optimum use of the dynamic (linear) range of the detector. The PSF shown in Figures 4 and 5 demonstrate this clearly: the detection limit without mask could have been about 1 mag better by increasing the exposure time. The AO performance has a large impact on the detection limit in that region as changing or bad image quality will directly influence the PSF wings. This is of course also true when using a coronographic mask and limits the use of the smallest mask sizes.

Further away from the bright source the detectivity is readout noise limited and using a larger mask size improves in that region the results. Again, the linear range of the detector should be used as well as possible.

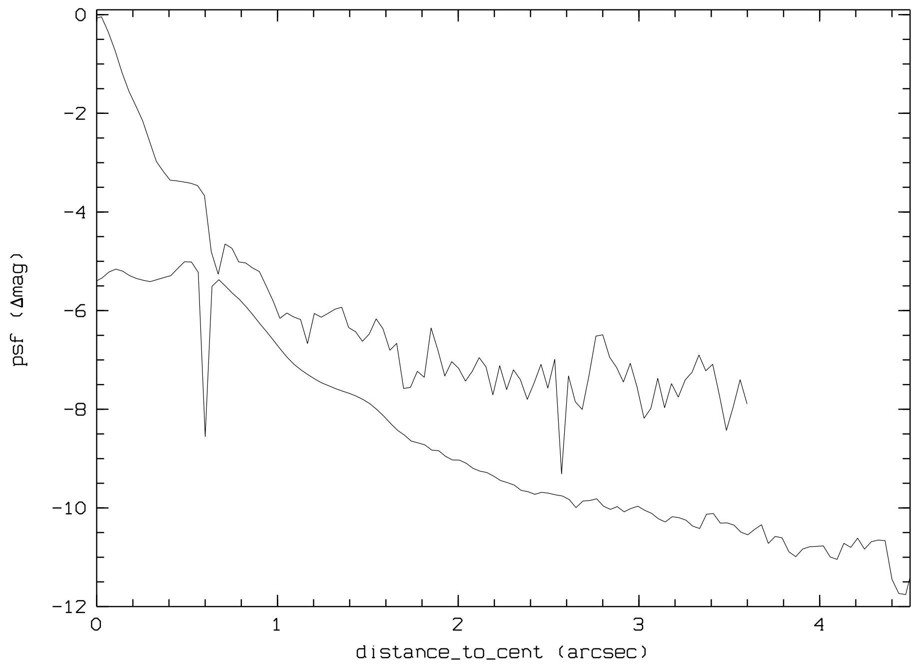

Figure 4 Observed detectivity (1σ) of the 0.″8 mask in the case of a H=8 star. The peak of the PSF without occulting mask was used as scaling reference and is represented by the upper line. Note, that the integration time of the PSF image was very short. This PSF is therefore dominated by readout noise. This demonstrates the necessity of using the whole dynamic range of the detector.
The lower line represents the profile of the occulted stellar light. The drop at ∼0.″6 (top) is due to the quadrant boundary gap of the INGRID CCD.

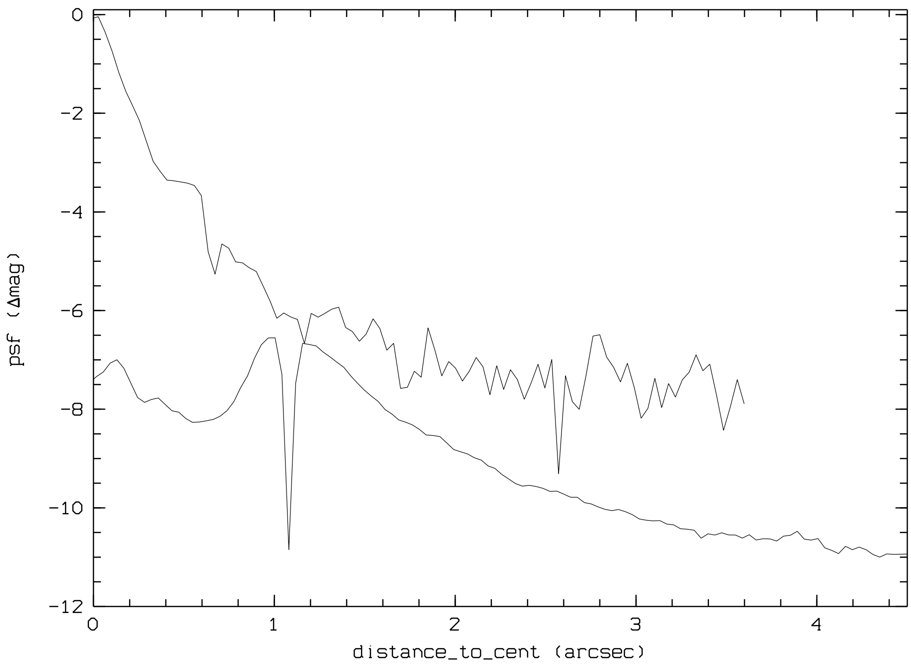

Figure 5 Same as Fig. 4 but for the 1.″6 mask. Again the quadrant boundary gap is visible.

4 Calibration Plan

In order to always asure the best performance of the OSCA system a monitoring of the system and a calibration plan should be performed. From the previous chapters the following monitoring/calibrations are proposed:
Before every OSCA run:

- obtain flatfields with each mask to monitor for
  - dust on the substrates;
  - additional features on substrates (degradation);
  - vignetting;
  - position of the masks on the CCD;
- simplex of NAOMI through the 1″target for the night;
- move OSCA in and out of the beam to test PSF reproducability and check for static abberations.

Best also during every OSCA run but at least once per semester:

- On-sky throughput measurements (degradation of substrates);
- monitor astrometric stability of the FOV (should be done every time after INGRID comes back from Cassegrain or alignment of the system was done).